Center-to-Limb variation of chromospheric fluctuations in UV diagnostics observed with IRIS

Momchil Molnar[1,2,3,4], Kevin Reardon[2,3], Steven Cranmer[3,4], Ivan Milic[5]

1. HAO/NCAR, Boulder, Colorado; 2. National Solar Observatory, Boulder, Colorado; 3. Department of Astrophysical and Planetary Sciences, University of Colorado, Boulder; 4. Laboratory for Atmospheric and Planetary Sciences, University of Colorado, Boulder; 5. Astronomical Observatory, Belgrade, Serbia

1. Different observational inclination angles provide us with a probe of the mix of longitudinal and transverse motions in the solar atmosphere

The observed Doppler velocity at any given inclination can be decomposed into contributions perpendicular and parallel to the local solar surface normal. By observing at different viewing angles, as encoded in the center-to-limb variation of the rms velocity amplitudes, we can estimate the relative amounts of vertical and transverse wave oscillations in different classes of solar features. Since transverse oscillations (where gravity is not a predominant restoring force) are thought to be predominantly due to Alfvén waves, we can use this information to estimate the amount of wave flux in these different wave modes, which is an important input parameter for many coronal heating models (Cranmer and Winebarger 2019). But this is valid under the questionable assumption that the magnetic field is predominantly vertical in the region of interest.

Figure 1: Decomposing the observed Doppler velocity V_{obs} in parallel and perpendicular components $V_\perp$ and $V_\parallel$, depending on the inclination.

$$\langle v_{obs}^2 \rangle = \langle v_\parallel^2 \rangle \cos^2\theta + \langle v_\perp^2 \rangle \sin^2\theta$$

$$\mu = \cos\theta$$
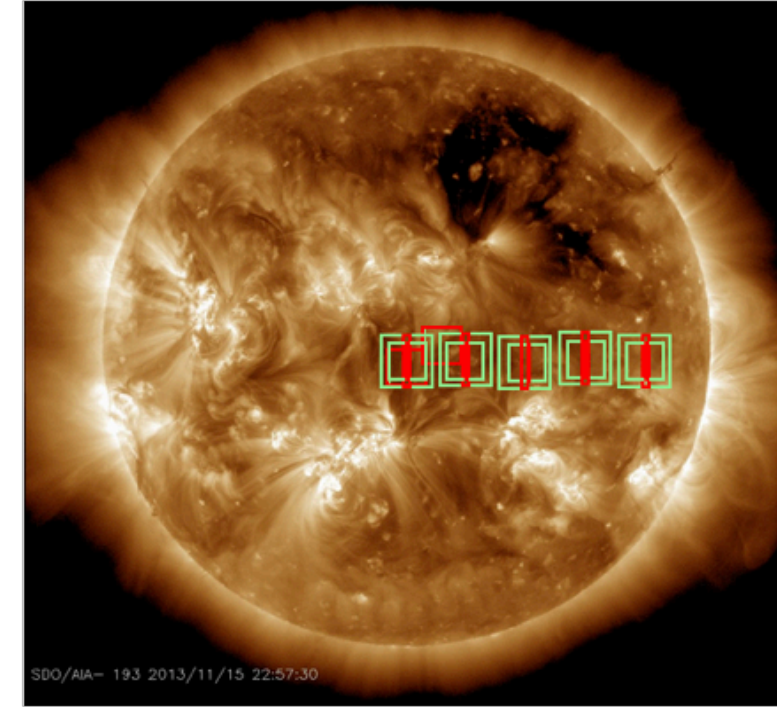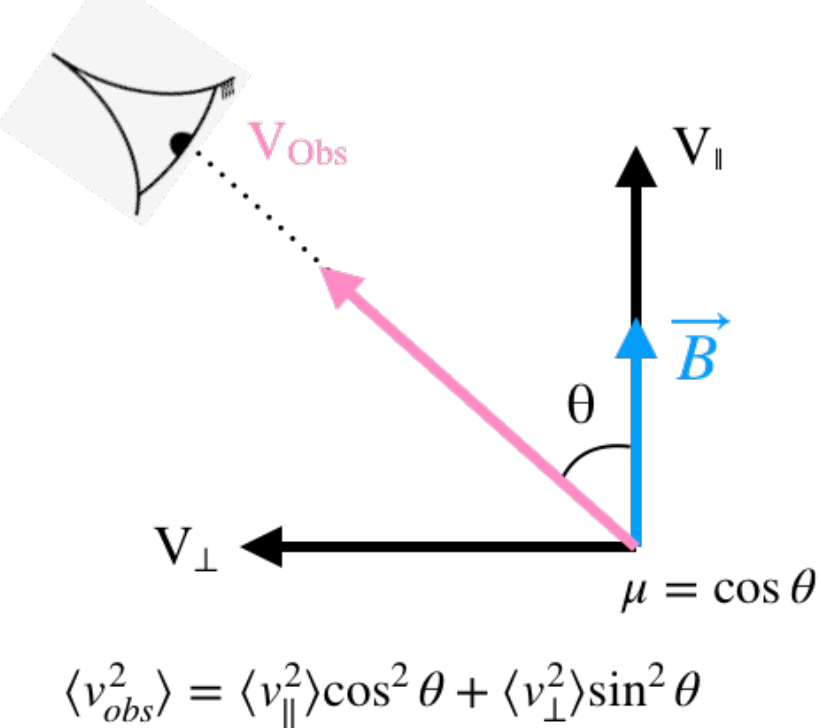
Figure 2: IRIS observing campaign of quiet sun regions at different inclinations on 16/17 November 2013.

Polar coronal hole Doppler velocity @ MnI 280.19 nm
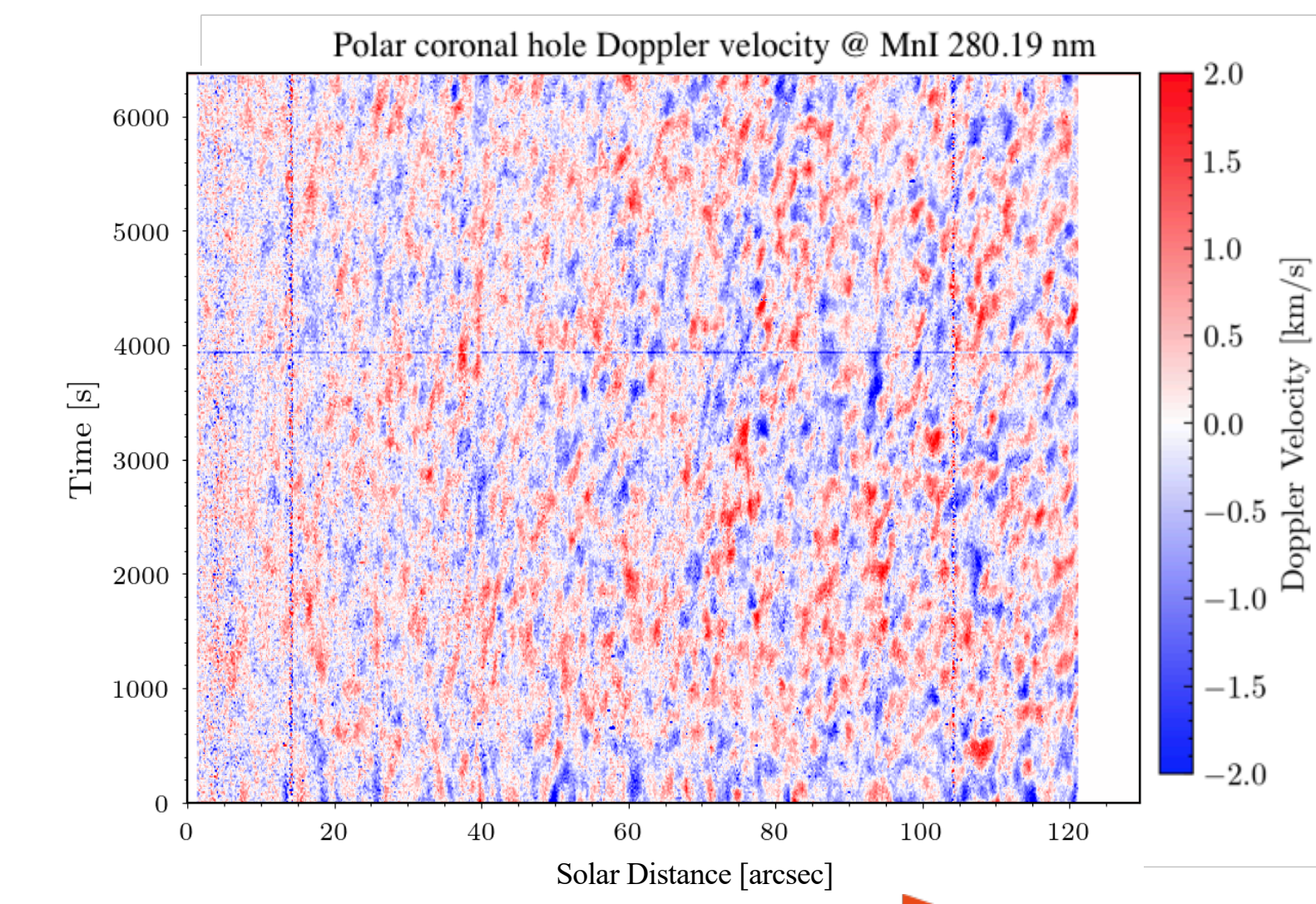
Figure 3: This time slice shows a Doppler velocity map of a polar coronal hole region, observed with IRIS in the Mn I 280.19 nm line, which samples the low chromosphere. The slit was oriented radially. We can see the trend of oscillations being less clearly pronounced towards the solar limb (left). This is consistent with other diagnostics formed in that region, but unlike the diagnostics formed in the upper chromosphere.
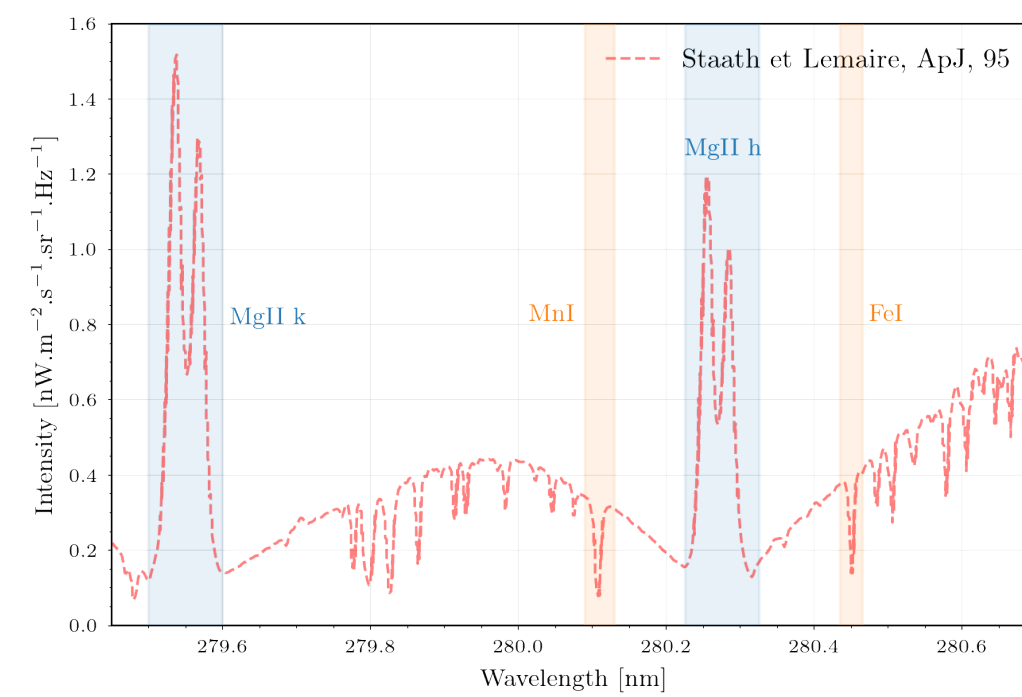
Figure 4: Observed region of the solar spectrum with IRIS used in this study. The Fe I line samples the photosphere (data omitted in this poster), Mn I line samples the lower chromosphere, whereas the Mg II h and k lines sample the higher chromosphere. (Pereira et al. 2013)

μ angle	Date ID [YYYYMMDD.HHMMSS]	Cadence, [s]	Lines used	Labels
1.00	20131116.073345	16.7	Mg II, Fe I, Mn I	IN
0.80	20131116.104845	16.7	Mg II, Fe I, Mn I	IN
0.60	20131117.044245	16.7	Mg II, Fe I, Mn I	IN
0.40	20131117.075745	16.7	Mg II, Fe I, Mn I	IN
0.20	20131117.111245	16.7	Mg II, Fe I, Mn I	IN
1.00	20140918.080253	5	Mg II, Fe I, Mn I	P
1.00	20140918.101908	9	Mg II, Fe I, Mn I	P
0.87	20131213.070938	9	Mg II, Fe I, Mn I	P
0.70	20200725.000137	9	Mg II, Fe I, Mn I	P
0.67	20131117.194238	9	Mg II, Fe I, Mn I	P
0.48	20140410.014930	9	Mg II, Fe I, Mn I	P
0.44	20130820.123133	4	Mg II, Fe I, Mn I	P
0.39	20160101.020028	17	Mg II, Fe I, Mn I	P
0.22	20160101.140128	17	Mg II, Fe I, Mn I	P
0.92	20170321.195128	16	Mg II, Fe I, Mn I	CH
0.82	20161107.025410	9.6	Mg II, Fe I, Mn I	CH
0.74	20161025.111933	9.6	Mg II, Fe I, Mn I	CH
0.64	20160321.210428	16	Mg II, Fe I, Mn I	CH
0.39	20140511.051421	9.6	Mg II, Fe I, Mn I	CH
0.25	20151008.194708	9.6	Mg II, Fe I, Mn I	CH

Table 1. IRIS observations used throughout this work. Labels: CH – coronal hole; P – plage; IN – internetwork.

Lines sampling two heights in the chromosphere show different center-to-limb trends of the line-of-sight velocity amplitudes. Is it a projection effect, or a signature of height-dependent Alfven wave generation?
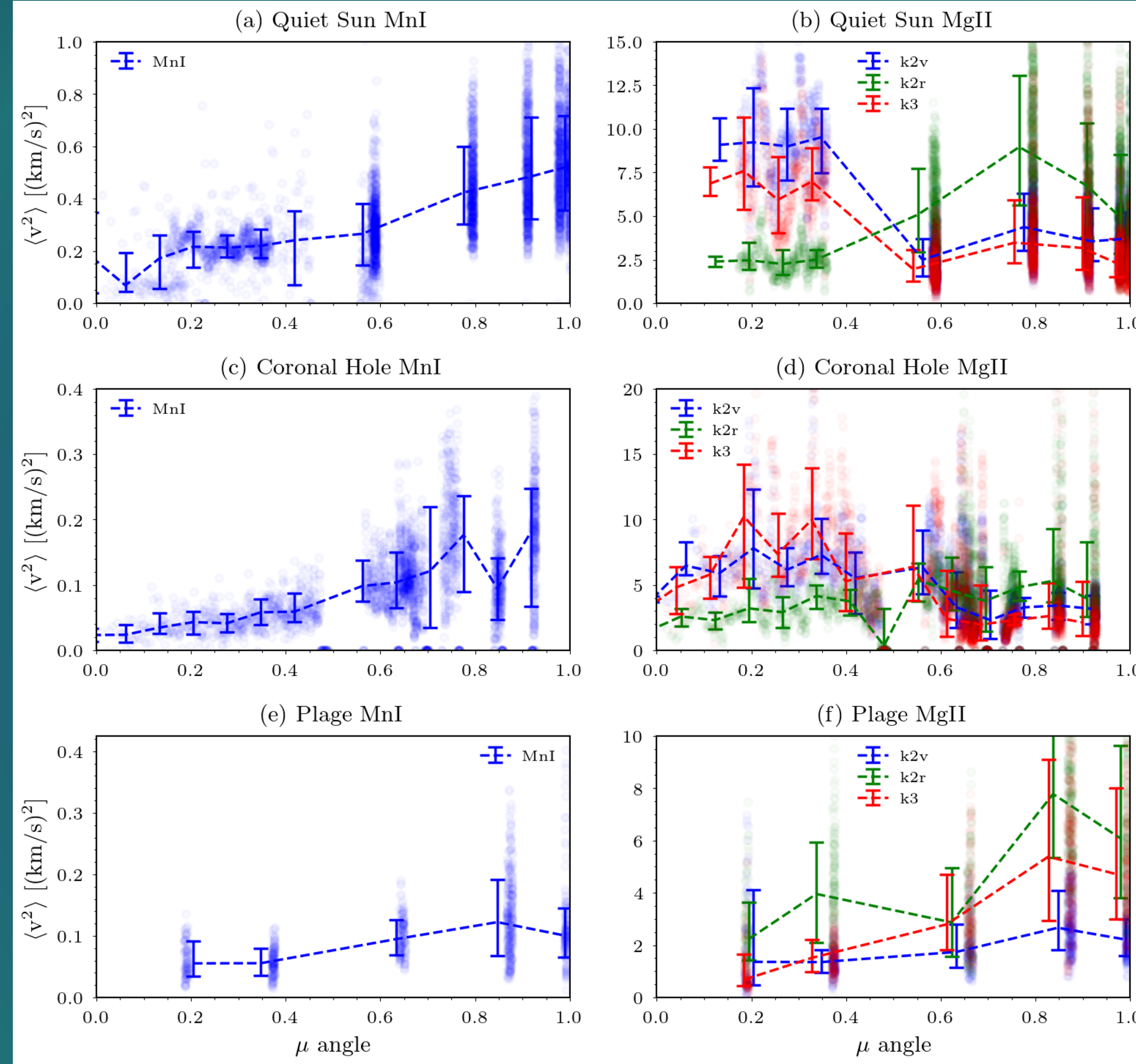
Figure 8: Center-to-limb variation of the observed Doppler velocity fluctuations in the Mn I 280.1 nm line, which samples the low chromosphere, and the Mg II k3 feature, which samples the upper chromosphere. Note the clear reduction in velocity amplitudes toward the solar limb for the Mn I, but much more uniform values across the disk for the Mg II line.

Online version of this poster:
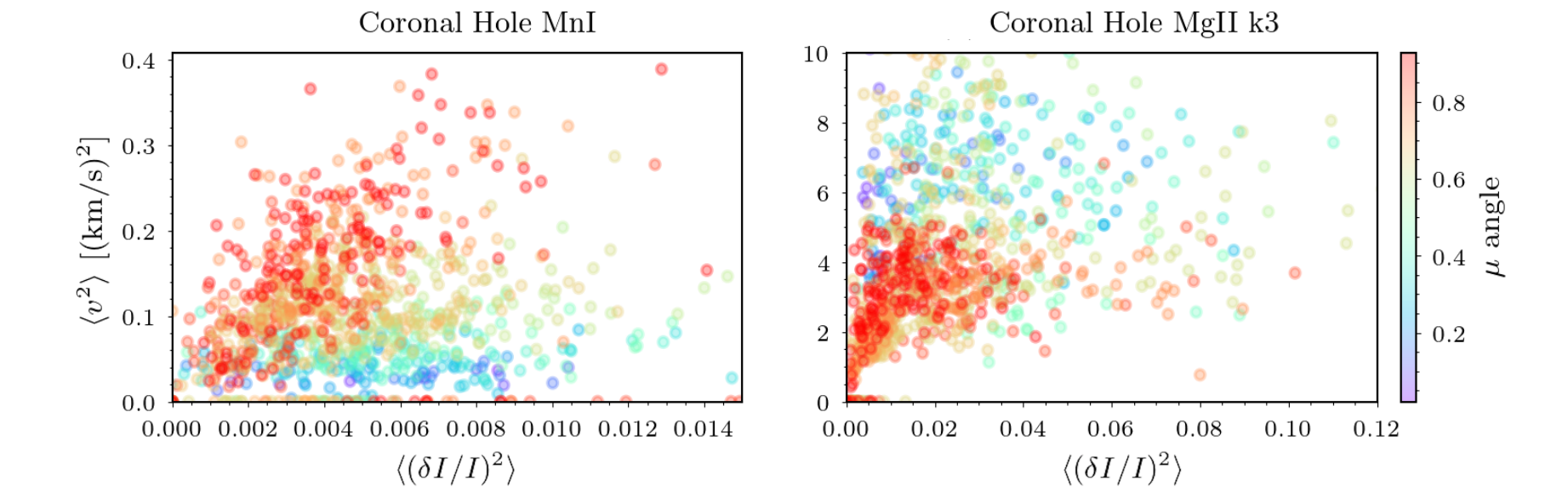
Figure 5: Figure 5: Correlation between intensity and Doppler velocity fluctuations, integrated between frequencies of 3 and 20 mHz, colored by the inclination angle. The observations are for a coronal for the Mn I line (left panel) and the Mg II k3 feature (right panel). The amplitudes of the intensity fluctuations do not seem to be strongly affected by the inclination angle, whereas the velocities show a strong decreasing trend with decreasing mu (increasing inclination angle).

2. Modeling the observed wave fluctuation CLV trends with Bifrost

Since the magnetic fields in the solar atmosphere are not perpendicular to the solar surface, we cannot interpret the observed longitudinal and transverse oscillations directly as MHD modes. We employ 3D rMHD Bifrost (Gudiksen et al. 2013) simulations to model the observed signatures of different mixture of transverse and longitudinal wave mixes to the magnetic field wave mixes.
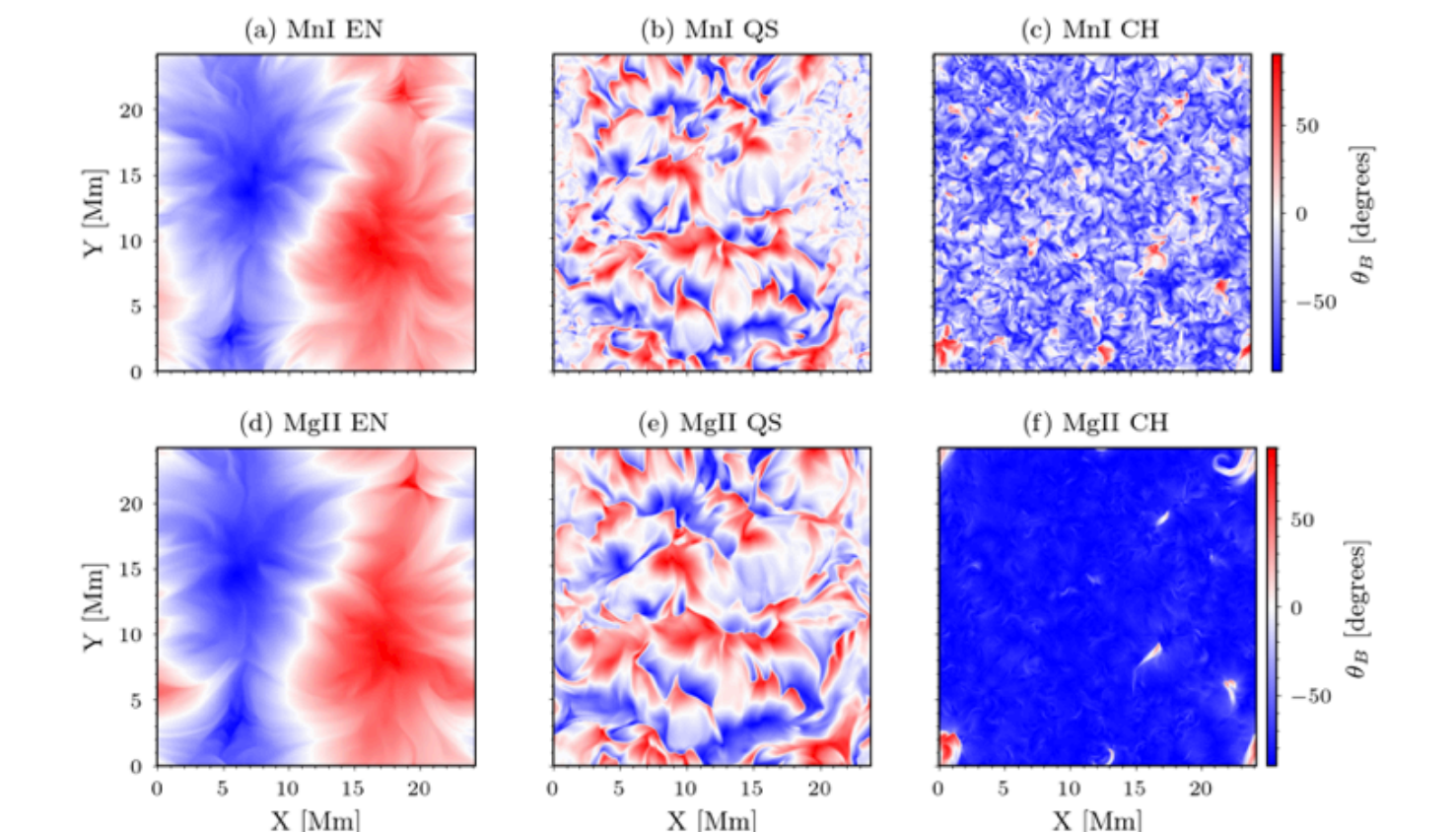
Figure 6: Magnetic field inclination at the average height of formation of the MnI 280.1 nm line (upper row) and the Mg II k3 feature (bottom row) in the Bifrost models for Enhanced Network model (panels (a) and (d)), Quiet Sun (panels (b) and (e)), and Coronal Hole model (panels (c) and (f)). White color denotes horizontal fields, whereas blue and red color shows vertical field orientation (Gudiksen et al. 2011). The largest difference in inclinations between the two lines are seen in the coronal hole model.
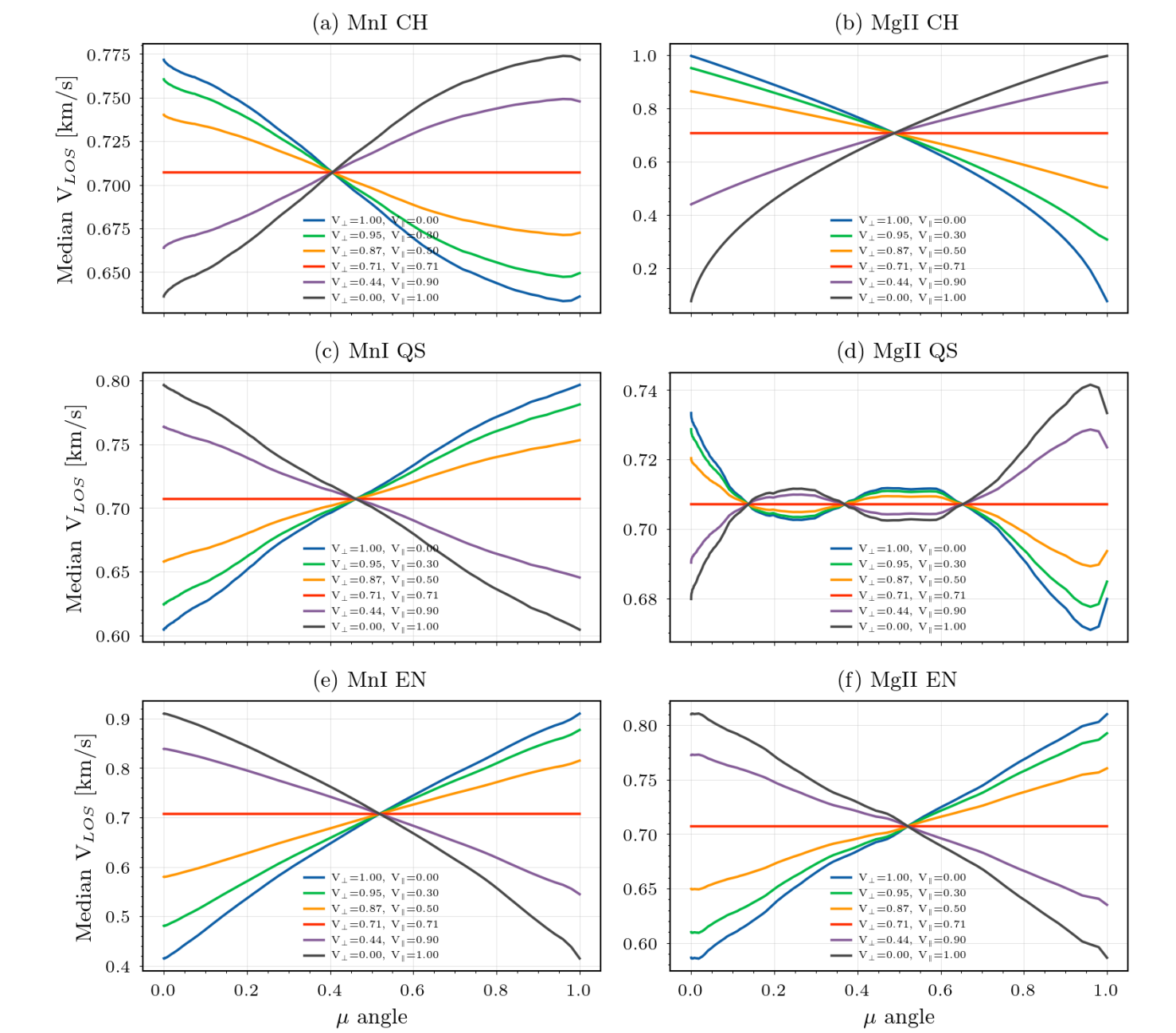
Figure 7: Expected center-to-limb trends of measured velocity fluctuations (for a total velocity amplitude on the Sun of 1 km/sec) based on the magnetic field topologies presented in Figure 6. The left column shows the results for the Mn I 280.1 nm line and the right column shows the results for the Mg II k3 feature. The different colors show models with differing relative amplitudes of $V_\perp$ and $V_\parallel$.

3. Conclusions and future work

We found that the center-to-limb variation of spectral diagnostics formed at different heights in the solar atmosphere show different trends in their center-to-limb RMS velocity amplitudes The Mn I 280.1 nm line, formed in the lower chromosphere exhibits decreasing wave amplitudes toward the limb, whereas the Mg II k3 feature exhibits an almost constant amplitude of wave fluctuations. Based on magnetic field geometry in the Bifrost simulations for the different solar regions, we can interpret this as increasing transverse wave amplitudes with height. The accurate estimate of the Alfvén wave amplitudes from the observations depends on multiple projection and radiative transfer effects, which we will address in our next step – synthesizing the observational signatures of the velocity field from realistic 3D MHD simulations, such as Bifrost at different inclination angles.

References: Cranmer and Winebarger, 2019, ARAA, 57, 157-187; Erdelyi et al., 1998, A&A, 337, 287; Gudiksen et al., 2011, A&A, 531, A154; M. Molnar, PhD thesis, 2022, University of Colorado, Boulder; Pereira et al., 2013, ApJ, 778:143; Peter et al, 1999, ApJ, 516, 490; Rao et al., 2022, MNRAS, 511, 1.